



Role of the malate–aspartate shuttle on the metabolic response to myocardial ischemia

Ming Lu^{a,d}, Lufang Zhou^{a,d}, William C. Stanley^{b,d,e}, Marco E. Cabrera^{a,b,c,d}, Gerald M. Saidel^{a,d}, Xin Yu^{a,d,*}

^a Department of Biomedical Engineering, Case Western Reserve University, Wickenden 427, 10900 Euclid Avenue, Cleveland, OH 44106, USA

^b Department of Physiology and Biophysics, Case Western Reserve University, Cleveland, OH, USA

^c Department of Pediatrics, Case Western Reserve University, Cleveland, OH, USA

^d Center for Modeling Integrated Metabolic Systems, Case Western Reserve University, Cleveland, OH, USA

^e Department of Medicine, Division of Cardiology, University of Maryland at Baltimore, Baltimore, MD, USA

ARTICLE INFO

Article history:

Received 14 March 2008

Received in revised form

23 May 2008

Accepted 23 May 2008

Available online 7 July 2008

Keywords:

Malate–aspartate shuttle

Metabolic compartmentation

Mathematical modeling

Myocardial ischemia

ABSTRACT

The malate–aspartate (M–A) shuttle provides an important mechanism to regulate glycolysis and lactate metabolism in the heart by transferring reducing equivalents from cytosol into mitochondria. However, experimental characterization of the M–A shuttle has been incomplete because of limitations in quantifying cytosolic and mitochondrial metabolites. In this study, we developed a multi-compartment model of cardiac metabolism with detailed presentation of the M–A shuttle to quantitatively predict non-observable fluxes and metabolite concentrations under normal and ischemic conditions *in vivo*. Model simulations predicted that the M–A shuttle is functionally localized to a subdomain that spans the mitochondrial and cytosolic spaces. With the onset of ischemia, the M–A shuttle flux rapidly decreased to a new steady state in proportion to the reduction in blood flow. Simulation results suggest that the reduced M–A shuttle flux during ischemia was not due to changes in shuttle-associated enzymes and transporters. However, there was a redistribution of shuttle-associated metabolites in both cytosol and mitochondria. Therefore, the dramatic acceleration in glycolysis and the switch to lactate production that occur immediately after the onset of ischemia is mediated by reduced M–A shuttle flux through metabolite redistribution of shuttle associated species across the mitochondrial membrane.

© 2008 Elsevier Ltd. All rights reserved.

1. Introduction

The compartmentation of metabolites and enzymes between and within cytosol and mitochondria plays an important role in the regulation of energy metabolism in coordination with cell function. Although the metabolic processes in the cytosol and mitochondria are controlled locally, communication between them is important to achieve optimal substrate utilization, as well as to maintain a balance between ATP production and utilization. In cardiomyocytes, cytosolic NADH is formed by glycolysis and lactate oxidation. To achieve maximal ATP production, cytosolic NADH must be transferred into the mitochondrial matrix to enter the electron transport chain, and cytosolic NAD⁺ must be regenerated to maintain glycolytic flux and lactate

conversion to pyruvate. It has been recognized that the inner mitochondrial membrane is impermeable to NADH (Purvis and Lowenstein, 1961). This led to the description of several NADH shuttle pathways including the malate–aspartate (M–A) shuttle, the α -glycerophosphate shuttle, the malate–citrate and fatty acid shuttles (Dawson, 1979). In the heart, the M–A shuttle is the dominant pathway with the rate of transporting NADH into mitochondria 10-fold or greater than that of NADH delivery via α -glycerophosphate shuttle (LaNoue et al., 1973; Safer et al., 1971; Scholz and Koppenhafer, 1995; Scholz et al., 1998; Rupert et al., 2000; Taylor et al., 2003).

The M–A shuttle comprises a transport–transamination–redox cycle in both cytosolic and mitochondrial domains. There are two antiporter proteins located in the inner membrane of the mitochondria, the glutamate–aspartate transporter (transporter I) and the malate– α -ketoglutarate transporter (transporter II). In transporter I, the efflux of aspartate from the mitochondria is accompanied by the stoichiometric entry of glutamate and proton into the mitochondria. Therefore, this electrogenically driven process is irreversible and the rate-controlling step of the M–A

* Corresponding author at: Department of Biomedical Engineering, Case Western Reserve University, Wickenden 427, 10900 Euclid Avenue, Cleveland, OH 44106, USA. Tel.: +1 216 368 3918; fax: +1 216 368 4969.

E-mail address: xin.yu@case.edu (X. Yu).

shuttle (LaNoue et al., 1974; LaNoue and Tischler, 1974). The exchange of malate and α -ketoglutarate through transporter II is driven by the concentration gradients of its substrates, and therefore is bidirectional (Safer, 1975; Sluse et al., 1972). By transferring reducing equivalents from cytosol into mitochondria, M–A shuttle provides an important mechanism to regulate metabolic activity in these two compartments (LaNoue and Williamson, 1971; LaNoue and Schoolwerth, 1979). In the healthy heart, the system operates with a net flow of electrons from the cytosol into the mitochondrial matrix that is sufficient to maintain both glycolysis and lactate oxidation, and thus prevent net lactate production. However, during ischemia there is a decrease in oxygen acceptance of electrons at Complex IV, which leads to inhibition of the transfer of NADH into the matrix via the M–A shuttle, resulting in a switch from lactate uptake to lactate production that is the biochemical hallmark of myocardial ischemia.

Experimental characterization of the M–A shuttle under both aerobic and ischemic conditions has been incomplete due to the limitations in measuring cytosolic and mitochondrial metabolite concentrations. The isolated mitochondria approach focuses on the efflux of metabolites from the mitochondria to an artificial cytosolic environment. This approach, therefore, has inherent limitations when attempting to elucidate the interactions between the two compartments that exist *in vivo*. Nuclear magnetic resonance (NMR) spectroscopy, such as ^{13}C NMR, is sensitive to metabolite transport across the mitochondria membrane in intact tissues (Yu et al., 1996; Griffin et al., 2000). However, its low temporal resolution renders it inadequate to study transient responses during sudden changes in perfusion or workload under pathophysiological conditions. Although pharmacological and physiological studies can describe phenomenological aspects of the shuttle, they provide limited mechanistic insight into the regulatory mechanisms at the subcellular level, particularly during the abrupt transition from normal aerobic conditions to ischemia.

As a complementary approach to experimental measurements, mathematical modeling of the interacting metabolites and enzymes involved in cardiac metabolism can be used to quantitatively predict non-observable fluxes and metabolite concentrations. With a physiologically based mathematical model that incorporates mechanistic details, computer simulations can be obtained for analysis of cardiac metabolic dynamics during normal and altered pathophysiological conditions. Such a computational model of cardiac energy metabolism that distinguishes transport and metabolic processes in blood, cytosol and mitochondria has been developed previously to simulate the dynamic metabolic responses to blood flow reduction and increased workload (Zhou et al., 2005b, 2006). This model includes key metabolic pathways such as glycolysis, fatty acid oxidation, the tricarboxylic acid (TCA) cycle and oxidative phosphorylation. The model predicted dynamic responses of chemical species and fluxes to altered pathophysiological conditions that cannot be reliably measured in cytosol and mitochondria. However, the role of M–A shuttle on metabolic responses to myocardial ischemia was not delineated due to the absence of a detailed presentation of M–A shuttle in this model.

In this study, the previous model of cardiac metabolism was expanded by including major components associated with the M–A shuttle, viz., redox and transamination reactions in both cytosol and mitochondria, as well as carrier-mediated transporters. Simulations with this improved model were compared with data from *in vivo* experiments performed in swine under normal flow and ischemic conditions (Salem et al., 2004; Stanley et al., 1992). By functionally localizing the M–A shuttle in a subdomain within the cardiomyocytes, simulation results suggest that

decreased shuttle flux after the onset of ischemia is due to the redistribution of shuttle-associated metabolites across the mitochondrial membrane.

2. Methods

2.1. Model development

To quantitatively elucidate the role of M–A shuttle on the regulation of cellular metabolism in cardiac tissue, we expanded the model of Zhou et al. (2005a) by including major components of the M–A shuttle (Fig. 1). The basic model represents the heart as a perfused tissue with a characteristic myocyte having distinct cytosolic and mitochondrial compartments. Chemical species are transported into the myocytes by convection in the blood capillaries while diffusion occurs between blood plasma and interstitial fluid. Since the characteristic time for capillary–interstitial transport is much shorter than that for convection through the capillaries, local chemical equilibrium between plasma and interstitial fluid can be assumed. Therefore, we considered the perfused tissue to have a single extracellular domain consisting of blood and interstitial fluid, which will be referred to as “blood.” Chemical species are transported by both passive and carrier-mediated mechanisms between (1) interstitial fluid and cytosol and (2) cytosol and mitochondria.

Within the cytosol and mitochondria, metabolic and transport processes can occur within and between distinct subdomains. Glycolysis is considered to occur in a subdomain of cytosol in which the metabolic components have a distinctive effective volume (Zhou et al., 2005a). Metabolic and transport processes of the M–A shuttle are considered to occur within a subdomain between cytosol and mitochondria. Within this M–A shuttle subdomain, the effective volume of the metabolic components is also distinct.

2.2. Dynamic mass balances

In response to alterations in pathophysiological conditions (e.g., ischemia), changes in metabolite concentrations in blood (*b*), cytosol (*c*) and mitochondria (*m*) are governed by dynamic mass balances in spatially lumped compartments. The dynamic mass balance equation for species *j* in capillary blood is

$$V_b \frac{dC_{bj}}{dt} = \frac{Q(C_{aj} - C_{bj})}{F} - J_{b-c,j} \quad (1)$$

where V_b is the effective volume of the blood domain, C_{bj} the concentration of species *j* in blood, C_{aj} the arterial concentration of species *j*, Q the blood flow, F a mixing fraction (Zhou et al., 2005a) and $J_{b-c,j}$ is the mass transport flux from blood to cytosol.

In the cytosolic domain, changes in metabolite concentrations are described by the metabolic reactions involved and transport processes across cellular and mitochondrial membranes, i.e.,

$$V_{cj} \frac{dC_{cj}}{dt} = R_{cj} + J_{b-c,j} - J_{c-m,j} \quad (2)$$

where V_{cj} is the effective volume of species *j* in the cytosol, C_{cj} the cytosolic concentration of species *j*, R_{cj} the metabolic reaction rate of species *j* and $J_{c-m,j}$ is the mass transport flux from cytosol to mitochondria.

Similarly, the mass balance equation for species *j* in the mitochondrial domain is

$$V_{mj} \frac{dC_{mj}}{dt} = R_{mj} + J_{c-m,j} \quad (3)$$

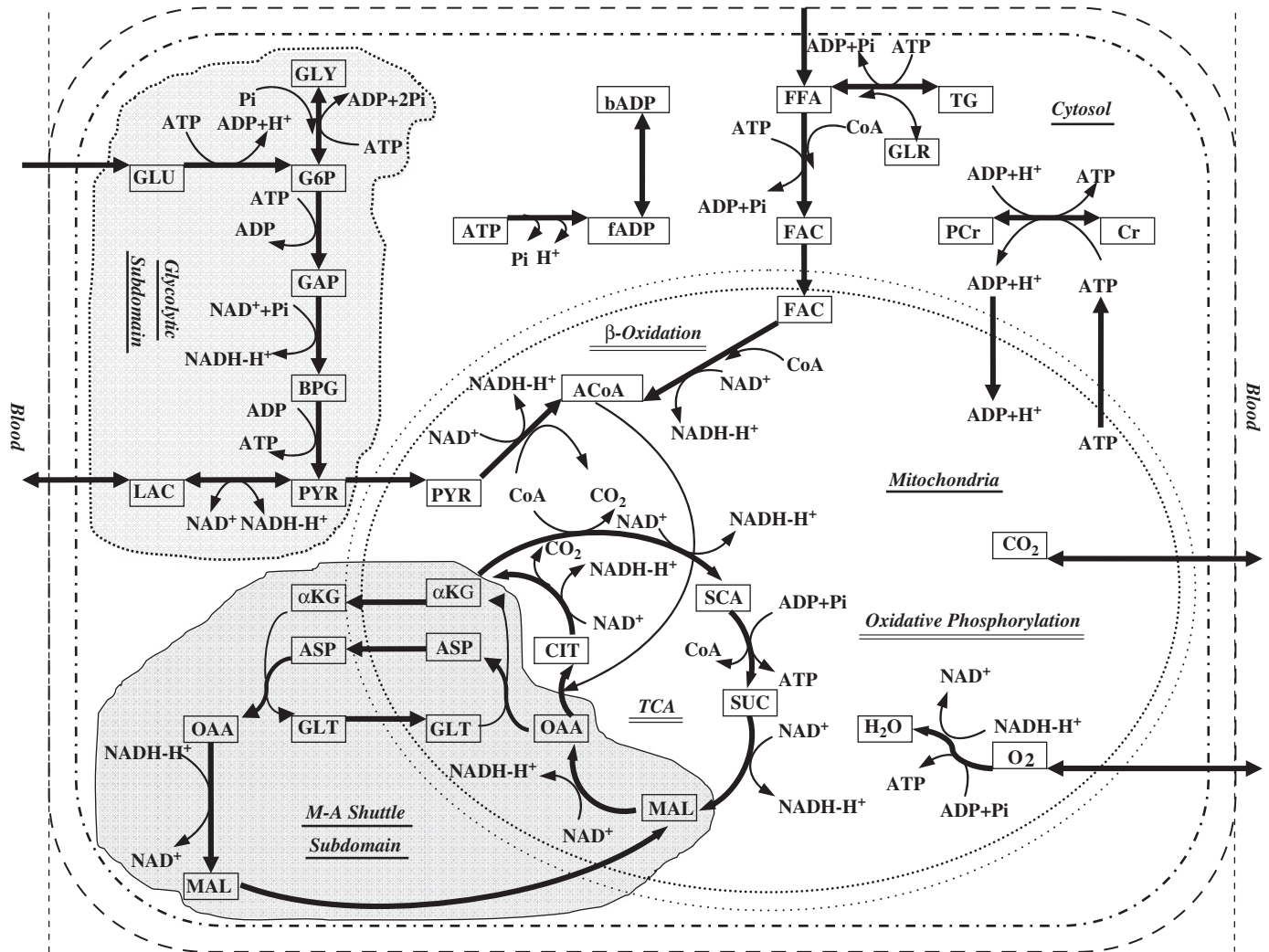


Fig. 1. Metabolic pathways in myocardium. This complex network incorporates most key biochemical reactions and pathways involved in cardiac metabolism including glycolysis, pyruvate oxidation, fatty acids oxidation, the tricarboxylic acid (TCA) cycle, oxidative phosphorylation and M-A shuttle. It also includes metabolite transport across cellular membrane and mitochondrial membrane. GLU, glucose; G6P, glucose-6-phosphate; GLY, glycogen; GAP, glyceraldehyde-3-phosphate; BPG, 1,3-bisphosphoglycerate; PYR, pyruvate; LAC, lactate; TG, triglyceride; GLR, glycerol; FFA, free fatty acid; FAC, fatty acyl-CoA; PCr, phosphocreatine; Cr, creatine; CIT, citrate; α -KG, α -ketoglutarate; SCA, succinyl-CoA; SUC, succinate; MAL, malate; OAA, oxaloacetate; ACoA, acetyl-CoA; bADP, bound ADP; fADP, free ADP; ASP, aspartate; GLT, glutamate.

where V_{mj} is the effective volume of species j in the mitochondrial domain, C_{mj} is the mitochondrial concentration of species j and R_{mj} is the net reaction rate.

2.3. Transport and metabolic fluxes

The transport and metabolic flux equations of this model (Appendix) are mostly identical with the previous model (Zhou et al., 2005a), with the inclusion of a detailed representation of the M-A shuttle. Our current model incorporates not only redox and transamination reactions in both cytosolic and mitochondrial compartments, but also two carrier-mediated transport processes (Table 1).

The net metabolic reaction rate R_{xj} is represented by the rates of production and utilization in domain x with a general Michaelis-Menten form as described previously (Zhou et al., 2005a).

The interdomain transport of metabolites occurs either through passive diffusion or by carrier-mediated transport processes. For the chemical species that are not associated with the M-A shuttle, passive diffusion between domains “ x ” and “ y ” is

Table 1
Major processes in the M-A shuttle

Reactions in cytosol	
Malate formation	Oxaloacetate+NADH+H ⁺ ↔ Malate+NAD ⁺
Transamination	α -Ketoglutarate+aspartate ↔ oxaloacetate+glutamate
Reactions in mitochondria	
Oxaloacetate formation	Malate+NAD ⁺ ↔ oxaloacetate+NADH+H ⁺
Transamination	Oxaloacetate+glutamate ↔ α -ketoglutarate+aspartate
Carrier-mediated transport processes	
Transporter I	Glutamate _(c) +aspartate _(m) → glutamate _(m) +aspartate _(c)
Transporter II	α -Ketoglutarate _(m) +malate _(c) ↔ α -ketoglutarate _(c) +malate _(m)

m and c represent mitochondria and cytosol, respectively. Transporter I is the unidirectional glutamate-aspartate transporter. Transporter II is the bidirectional malate- α -ketoglutarate transporter.

described by

$$J_{x \rightarrow y}^p = \lambda_{x \rightarrow y} (C_{xj} - \sigma_{x \rightarrow y} C_{yj}) \quad (4)$$

where $J_{x \rightarrow yj}^p$ is the passive transport flux, $\lambda_{x \rightarrow yj}$ is the membrane transport coefficient that is governed by membrane permeability and effective surface area, C_{xj} and C_{yj} are the concentrations of species j in domains “x” and “y”, respectively, and $\sigma_{x \rightarrow yj}$ is the partition coefficient of species j between domains “x” and “y”.

The rate of carrier-mediated transport is expressed by a Michaelis–Menten equation

$$J_{x \rightarrow yj}^f = \frac{T_{x \rightarrow yj} C_{xj}}{M_{x \rightarrow yj} + C_{xj}} \quad (5)$$

where $J_{x \rightarrow yj}^f$ is the carrier-mediated transport flux, C_{xj} is the concentration of species j in domain “x”, $T_{x \rightarrow yj}$ and $M_{x \rightarrow yj}$ are the transport rate and affinity coefficients, respectively.

Metabolic reactions and transport processes for M–A shuttle associated species are listed in Table 2. Flux through the unidirectional transporter I is described as

$$J_{GLT:c \rightarrow m, ASP:m \rightarrow c}^f = \frac{T_{GLT:c \rightarrow m, ASP:m \rightarrow c}}{1 + [(M_{GLT:c \rightarrow m}/C_{c,GLT}) + (M_{ASP:m \rightarrow c}/C_{m,ASP})]} \quad (6)$$

where $C_{c,GLT}$ and $C_{m,ASP}$ are cytosolic glutamate and mitochondrial aspartate concentrations, respectively, $T_{GLT:c \rightarrow m, ASP:m \rightarrow c}$ is the normalized unidirectional transport rate coefficient, $M_{GLT:c \rightarrow m}$ and $M_{ASP:m \rightarrow c}$ are unidirectional transport affinity coefficients for glutamate and aspartate, respectively. In this expression, we have assumed that the transport rate coefficient in the opposite direction, $T_{GLT:m \rightarrow c, ASP:c \rightarrow m}$, is sufficiently small to consider the flux rate in the opposite direction negligible.

Flux through the bidirectional transporter II is described by fluxes in both directions

$$J_{MAL:c \leftrightarrow m, aKG:m \leftrightarrow c}^f = J_{MAL:c \rightarrow m, aKG:m \rightarrow c}^f - J_{MAL:m \rightarrow c, aKG:c \rightarrow m}^f$$

with

$$J_{MAL:c \rightarrow m, aKG:m \rightarrow c}^f = \frac{T_{MAL:c \rightarrow m, aKG:m \rightarrow c}}{[1 + (M_{MAL:c \rightarrow m}/C_{c,MAL}) + (M_{aKG:m \rightarrow c}/C_{m,aKG})]} \quad (7)$$

and

$$J_{MAL:m \rightarrow c, aKG:c \rightarrow m}^f = \frac{T_{MAL:m \rightarrow c, aKG:c \rightarrow m}}{[1 + (M_{MAL:m \rightarrow c}/C_{m,MAL}) + (M_{aKG:c \rightarrow m}/C_{c,aKG})]} \quad (8)$$

where $J_{MAL:c \rightarrow m, aKG:m \rightarrow c}^f$ and $J_{MAL:m \rightarrow c, aKG:c \rightarrow m}^f$ are forward and backward transport fluxes, respectively. $C_{c,MAL}$, $C_{m,MAL}$, $C_{c,aKG}$ and $C_{m,aKG}$ are malate and α -ketoglutarate concentrations in cytosol and mitochondria, respectively. $T_{MAL:c \leftrightarrow m, aKG:m \leftrightarrow c}$ is the maximal bidirectional transport rate coefficient, and $M_{MAL:c \leftrightarrow m}$ and $M_{aKG:m \leftrightarrow c}$ are the bidirectional transport affinity coefficients for malate and α -ketoglutarate, respectively.

Table 2

Net reaction and transport rates of M–A shuttle associated metabolites

Metabolites	Cytosolic domain	Mitochondria domain
MAL	$\phi_{OAA-NADH \leftrightarrow MAL-NAD}^c - J_{MAL:c \leftrightarrow m, aKG:m \leftrightarrow c}^f$	$J_{MAL:c \leftrightarrow m, aKG:m \leftrightarrow c}^f + \phi_{SUC \rightarrow MAL}^m - \phi_{MAL-NAD \leftrightarrow OAA-NADH}^m$
OAA	$\phi_{aKG-ASP \leftrightarrow OAA-GLT}^c - \phi_{OAA-NADH \leftrightarrow MAL-NAD}^c$	$\phi_{MAL-NAD \leftrightarrow OAA-NADH}^m - \phi_{OAA-GLT \leftrightarrow aKG-ASP}^m - \phi_{ACoA \rightarrow CIT}^m$
ASP	$J_{GLT:c \rightarrow m, ASP:m \rightarrow c}^f - \phi_{aKG-ASP \leftrightarrow OAA-GLT}^c$	$\phi_{OAA-GLT \leftrightarrow aKG-ASP}^m - J_{GLT:c \rightarrow m, ASP:m \rightarrow c}^f$
α KG	$J_{MAL:c \leftrightarrow m, aKG:m \leftrightarrow c}^f - \phi_{aKG-ASP \leftrightarrow OAA-GLT}^c$	$\phi_{OAA-GLT \leftrightarrow aKG-ASP}^m + \phi_{CIT \rightarrow aKG}^m - \phi_{aKG \rightarrow SCA}^m - J_{MAL:c \leftrightarrow m, aKG:m \leftrightarrow c}^f$
GLT	$\phi_{aKG-ASP \leftrightarrow OAA-GLT}^c - J_{GLT:c \rightarrow m, ASP:m \rightarrow c}^f$	$J_{GLT:c \rightarrow m, ASP:m \rightarrow c}^f - \phi_{OAA-GLT \leftrightarrow aKG-ASP}^m$

MAL, OAA, ASP, α KG, GLT, SUC, ACoA, CIT and SCA are malate, oxaloacetate, aspartate, α -ketoglutarate, glutamate, succinate, acetyl-CoA, citrate, and succinyl-CoA, respectively. ϕ and J are the reaction and transport fluxes, respectively. f refers to facilitated transport. The subscripts or superscripts c and m refer to cytosol and mitochondria, respectively.

The reversible reactions in the M–A shuttle in the form of



are expressed as a combination of forward and backward fluxes, i.e.,

$$\phi_{x-y \leftrightarrow v-w}^k = \phi_{x-y \rightarrow v-w}^k - \phi_{v-w \rightarrow x-y}^k$$

where k indicates the subcellular compartment in which the reaction occurs ($k = c$ or m). The forward and backward fluxes are described by Michaelis–Menten equations

$$\phi_{x-y \rightarrow v-w}^k = \frac{V_{x-y \rightarrow v-w}^k (C_{k,x} C_{k,y} / K_{x-y \rightarrow v-w}^k)}{[1 + (C_{k,x} C_{k,y} / K_{x-y \rightarrow v-w}^k) + (C_{k,v} C_{k,w} / K_{v-w \rightarrow x-y}^k)]} \quad (10)$$

$$\phi_{v-w \rightarrow x-y}^k = \frac{V_{v-w \rightarrow x-y}^k (C_{k,v} C_{k,w} / K_{v-w \rightarrow x-y}^k)}{[1 + (C_{k,x} C_{k,y} / K_{x-y \rightarrow v-w}^k) + (C_{k,v} C_{k,w} / K_{v-w \rightarrow x-y}^k)]} \quad (11)$$

where $C_{k,x}$, $C_{k,y}$, $C_{k,v}$ and $C_{k,w}$ are metabolite concentrations in the corresponding subcellular compartment, $V_{x-y \rightarrow v-w}^k$ and $V_{v-w \rightarrow x-y}^k$ are maximal forward and backward reaction rates, respectively, $K_{x-y \rightarrow v-w}^k$ and $K_{v-w \rightarrow x-y}^k$ are forward and backward reaction equilibrium coefficients, respectively.

2.4. Parameter estimation and model simulation

Flux balance analysis was applied to obtain steady-state flux values for shuttle reactions and transport processes under normal blood flow. Concentrations of shuttle-associated metabolites were taken from literature (Panchal et al., 2000, 2001; Stanley et al., 2003; Gibala et al., 1997; Caputo et al., 1998) and are listed in Table 3. Concentrations of other metabolites and flux values were

Table 3

Cytosolic and mitochondrial concentrations of M–A shuttle associated metabolites

Species	Total concentration (C_{ij})	C_{cj}	Mass $_{cj}$ %	C_{mj}	Mass $_{mj}$ %
Malate	0.160 (a, b, c)	0.012	5	0.940	95 (d)
α -Ketoglutarate	0.030 (d)	0.002	5	0.170	95 (d)
Oxaloacetate	0.003 (e)	0.001	5	0.017	95 (d)
Glutamate	7.680 (f)	9.874	90	4.518	10 ^a
Aspartate	1.330 (f)	1.710	90	0.782	10 ^a

C_{ij} , C_{cj} and C_{mj} are total, cytosolic and mitochondrial concentrations ($\mu\text{mol/g}$ wet weight), respectively. Mass $_{cj}$ and Mass $_{mj}$ are mass fractions in cytosol and mitochondria, respectively. References are listed in parentheses: a (Panchal et al., 2000); b (Panchal et al., 2001); c (Stanley et al., 2003); d (Zhou et al., 2005a); e (Gibala et al., 1997); f (Caputo et al., 1998).

^a Assumption made in current research.

the same as those of an earlier model (Zhou et al., 2005a). The values of reaction equilibrium coefficients and the transport affinity coefficients were chosen as the same magnitude of the corresponding concentration values. Since the flux values are constrained by the entire network of reactions, all the other kinetic parameters such as maximal reaction rates and normalized transport rate coefficients were determined by flux balance analysis. Kinetic parameters that were estimated by simulation and comparison with experimental data from literature are listed in Tables 4 and 5.

Each domain volume in the mass balance equations was represented as effective volume, i.e., V_j/V_{cell} , where j represents blood, cytosol or mitochondria domains and V_{cell} is the total cell volume. Metabolites associated with glycolysis or M–A shuttle are assigned distinct effective volumes (Appendix). To investigate the effect of localization of the M–A shuttle, simulations in response to blood flow reduction were performed with or without a shuttle subdomain. With a subdomain, the effective volumes of the species j in the cytosol (c) or mitochondria (m) are related to the cell volume as $V_{cj}/V_{cell} = V_{mj}/V_{cell} = f_j$.

Once steady-state fluxes at normal conditions were determined, metabolic responses to mild, moderate and severe ischemia were simulated to investigate the changes in M–A shuttle flux and its role in regulating cytosolic and mitochondrial metabolism. Specifically, at the fifth minute of simulation blood flow (Q) was reduced linearly from its normal value of 1.0 ml/min/g to 0.7, 0.4 and 0.1 ml/min/g over a period of 60 s, corresponding to mild (30%), moderate (60%) and severe (90%) ischemia, respectively. Simulations were performed by solving the model equations using DLSODE, a robust implicit integrator for stiff and sparse systems (<http://www.llnl.gov/CASC/odepack/software/dlsode.f>).

Table 4
M–A shuttle related reaction fluxes and parameters under normal conditions

Reactions	Net flux	Kinetic parameters			
		$V_{x-y \rightarrow v-w}$	$K_{x-y \rightarrow v-w}$	$V_{v-w \rightarrow x-y}$	$K_{v-w \rightarrow x-y}$
Malate formation	0.73	2.40	0.00005	0.077	0.005
Oxaloacetate formation	2.58	8.33	0.380	0.260	0.0007
Cytosolic transamination	0.73	2.07	0.003	0.082	0.010
Mitochondrial transamination	0.73	2.25	0.076	0.078	0.133

$V_{x-y \rightarrow v-w}$ and $V_{v-w \rightarrow x-y}$ are maximal forward and backward reaction rates ($\mu\text{mol/min/g}$ wet weight), respectively. $K_{x-y \rightarrow v-w}$ and $K_{v-w \rightarrow x-y}$ are forward and backward reaction equilibrium coefficients ($\mu\text{mol/g}$ wet weight), respectively. Unit for net flux is $\mu\text{mol/min/g}$ wet weight.

Table 5
M–A shuttle related transport fluxes and parameters under normal conditions

Transporters	Net flux	Parameters
Transporter I	0.73	$T_{GLT:c \rightarrow m, ASP:m \rightarrow c} = 2.197$, $M_{GLT:c \rightarrow m} = 10.0$, $M_{ASP:m \rightarrow c} = 0.78$
Transporter II	0.73	$T_{MAL:c \leftrightarrow m, \alpha KG:m \leftrightarrow c} = 2.270$, $M_{MAL:c \leftrightarrow m} = 0.01$, $M_{\alpha KG:m \leftrightarrow c} = 0.2$

Transporters I and II are the unidirectional glutamate-aspartate (GLT-ASP) transporter and the bidirectional malate- α -ketoglutarate (MAL- α -KG) transporter, respectively. $T_{GLT:c \rightarrow m, ASP:m \rightarrow c}$ and $T_{MAL:c \leftrightarrow m, \alpha KG:m \leftrightarrow c}$ are the normalized transport rate coefficients ($\mu\text{mol/min/g}$ wet weight) for transporters I and II, respectively. $M_{GLT:c \rightarrow m}$, $M_{ASP:m \rightarrow c}$, $M_{MAL:c \leftrightarrow m}$ and $M_{\alpha KG:m \leftrightarrow c}$ are the corresponding affinity coefficients ($\mu\text{mol/g}$ wet weight) for glutamate, aspartate, malate and α -ketoglutarate, respectively. The subscripts c and m refer to cytosol and mitochondria, respectively. Unit for net flux is $\mu\text{mol/min/g}$ wet weight.

3. Results

3.1. Responses of glycogen and lactate and model validation

As shown in Fig. 2a, moderate ischemia triggered a net glycogen breakdown that led to an 85% reduction in glycogen concentration. This response was in agreement with *in vivo* experimental data from a well-characterized swine model subjected to 60% ischemia (Salem et al., 2004). Also consistent with experimental data, myocardium switched from net lactate uptake to production and reached a steady-state release rate of $0.44 \mu\text{mol/min/g}$ ww (wet weight) with the onset of ischemia (Fig. 2b). Thus, expanding our previous model to incorporate the complex reactions of the M–A shuttle resulted in simulations of the myocardial metabolic response to ischemia that closely matched experimental data.

3.2. Responses of cytosolic and mitochondrial redox states

The impact of effective volumes for shuttle-associated species on changes in cytosolic and mitochondrial redox states (NADH/NAD^+) were simulated in response to moderate ischemia.

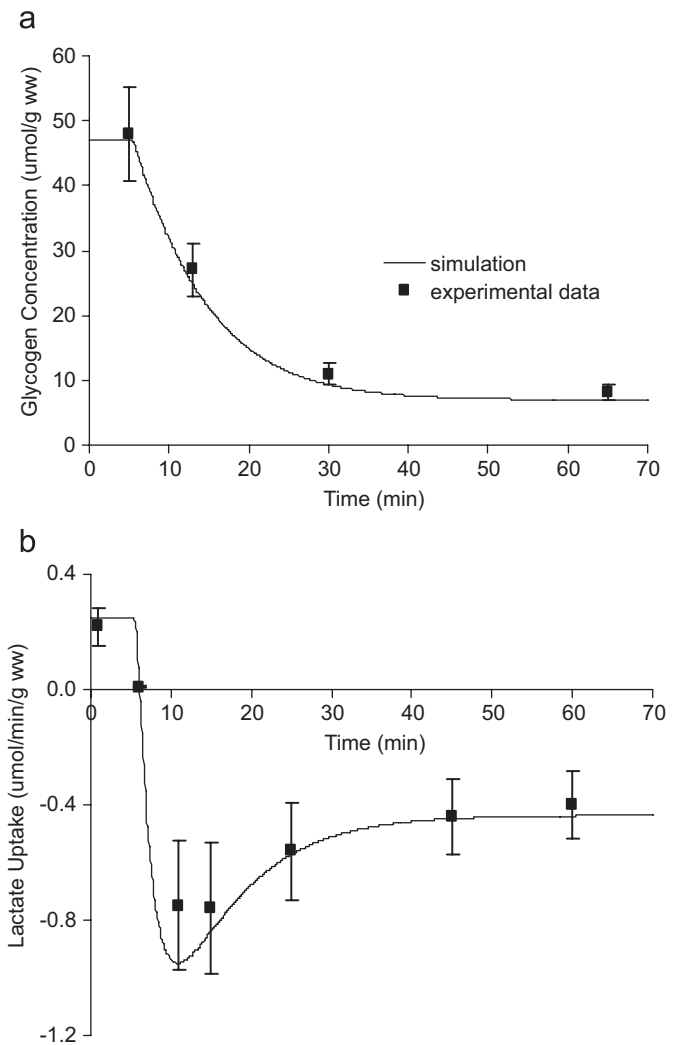


Fig. 2. Comparison of experimental data with simulated metabolic responses to moderate ischemia (60% coronary blood flow reduction). (a) Changes in glycogen concentration, (b) changes in lactate uptake. Experimental data are from *in vivo* swine study subjected to 60% blood flow reduction (Salem et al., 2004). Decrease in blood flow started at the fifth minute of simulation.

As shown in Fig. 3, different values of effective volume led to different time courses in response to ischemia. In the absence of a distinct M–A shuttle subdomain, both mitochondria and cytosol showed a two-stage increase in redox state. Even with a relatively large effective volume ($f_j = 0.3$), this two-stage increase still existed. With an effective volume of the M–A shuttle subdomain, ranging from 0.01 to 0.05, simulations showed a continuous increase in cytosolic redox state before it reached its maximum. Mitochondrial redox state also increased monotonically until it reached steady state.

Simulations with the effective M–A shuttle volume of 0.05 showed that cytosolic and mitochondrial redox states (NADH/NAD^+) responded differently to ischemia. Cytosolic redox state showed a biphasic transition to new steady state. It increased rapidly from an initial value of 0.1 to peak values of 0.75, 1.39 and 5.0 in response to mild, moderate and severe ischemia, followed by a decrease to steady-state values of 0.44, 0.52 and 1.3,

respectively (Fig. 4a). In contrast, mitochondrial redox state showed a rapid, monophasic increase following the onset of ischemia (Fig. 4b).

3.3. Shuttle activity in response to ischemia

The M–A shuttle flux via transporter I decreased rapidly with the onset of ischemia with an effective M–A shuttle volume of 0.05 (Fig. 5a). The decrease in the shuttle flux was greater with a larger reduction in blood flow. The responses of shuttle-associated metabolites to moderate ischemia are shown in Fig. 5b–f. With the onset of ischemia, there was a rapid but modest increase in glutamate concentration in both cytosol (from 9.9 to 11.6 $\mu\text{mol/g ww}$) and mitochondria (from 4.5 to 5.2 $\mu\text{mol/g ww}$) (Fig. 5b). Aspartate and oxaloacetate decreased by about 90% in both compartments (Fig. 5c and f). Malate concentration increased by ninefold in cytosol with a biphasic transition, but decreased by 80% in mitochondria (Fig. 5d). As a result, total tissue concentration of malate remained unaltered (0.15 $\mu\text{mol/g ww}$

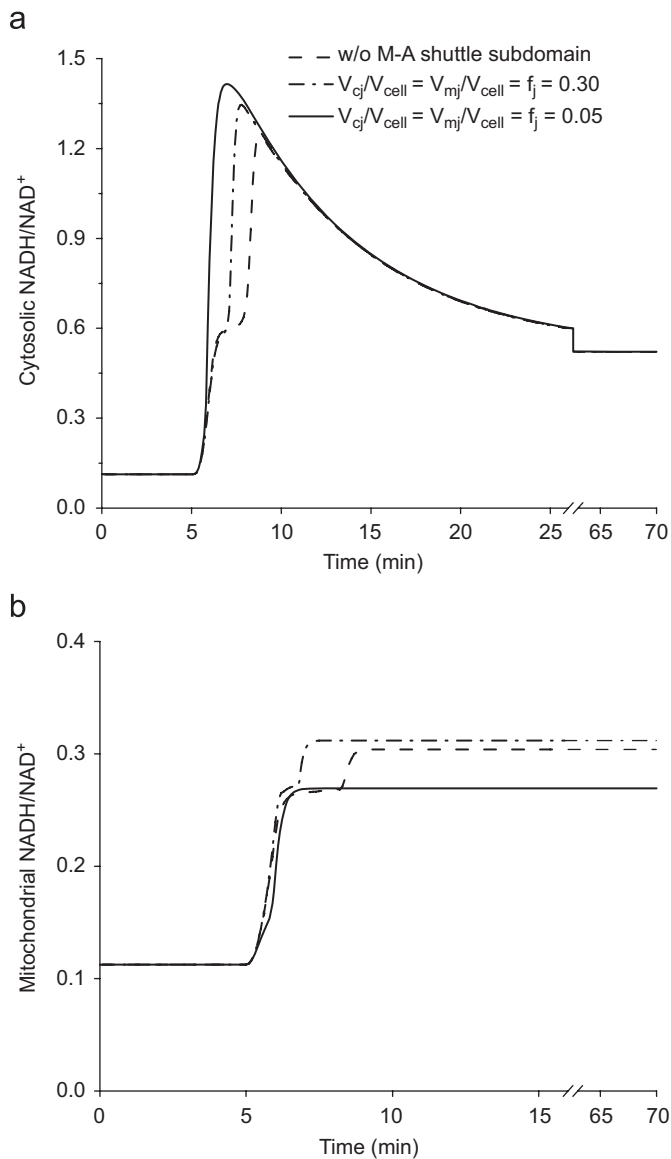


Fig. 3. Effects of M–A shuttle subdomain volume on cytosolic and mitochondrial response to moderate ischemia (60% reduction in flow). (a) Cytosolic NADH/NAD^+ dynamics, (b) mitochondrial NADH/NAD^+ dynamics. $V_{cj}/V_{cell} = V_{mj}/V_{cell} = f_j$ represents the effective volume of the M–A shuttle subdomain; j , species associated with M–A shuttle and “w/o M–A shuttle subdomain” represents no distinct effective volume for shuttle-associated species.

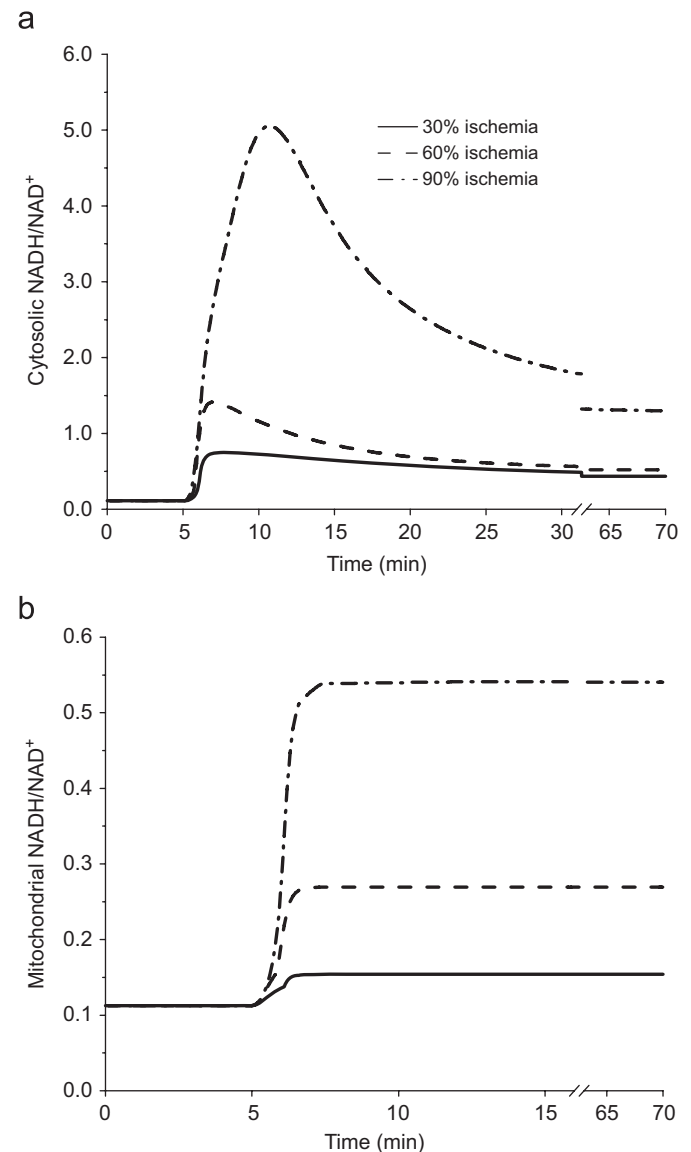


Fig. 4. Computer-simulated responses of cytosolic (a) and mitochondrial (b) redox state during mild, moderate and severe ischemia (30%, 60% and 90% coronary blood flow reduction).

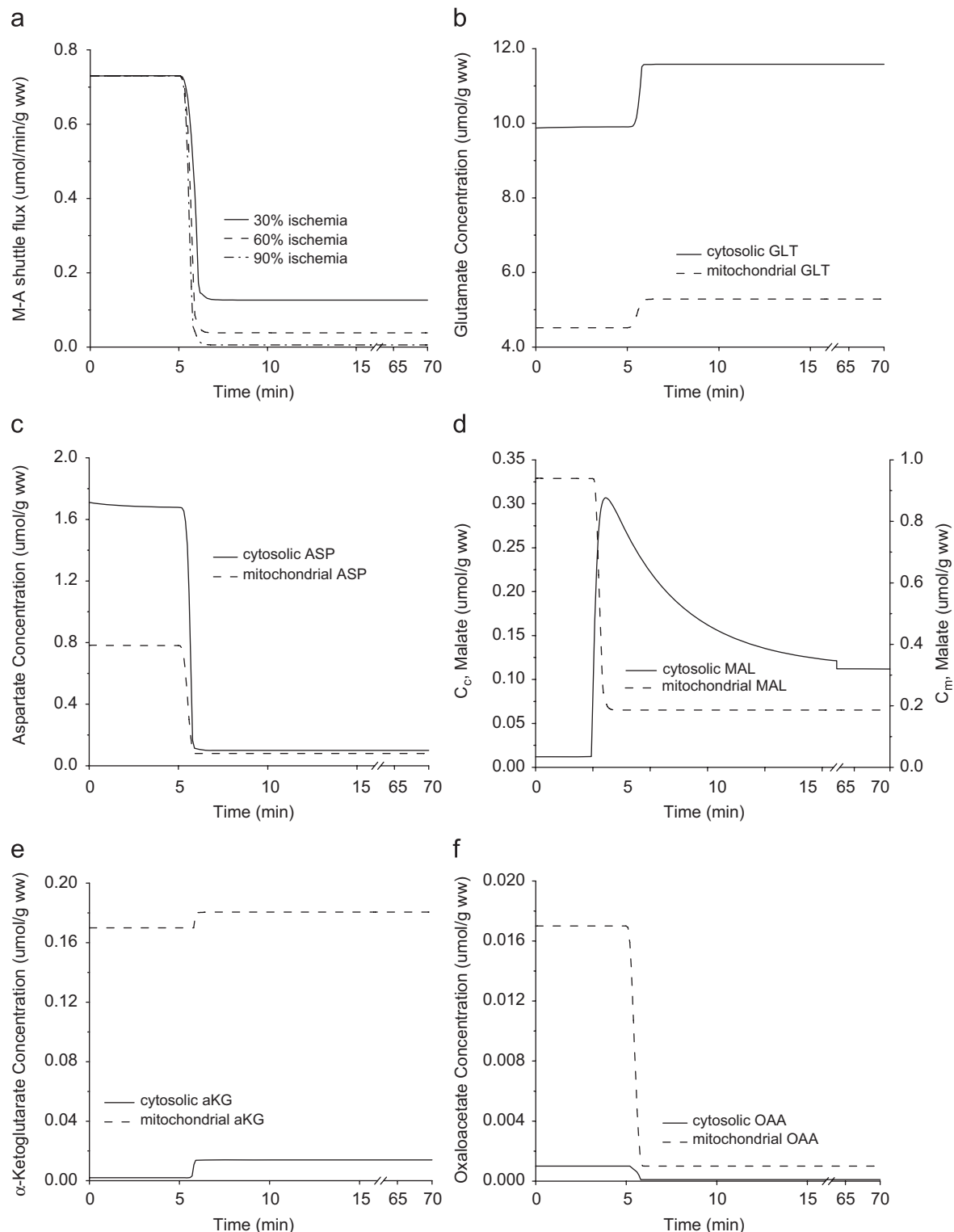


Fig. 5. Response of M–A shuttle to ischemia. (a) Computer-simulated changes of M–A shuttle flux in response to mild, moderate and severe ischemia (30%, 60% and 90% reduction in coronary blood flow, respectively); the dynamic responses of glutamate (GLT) (b), aspartate (ASP) (c), malate (MAL) (d), α -ketoglutarate (α KG) (e) and oxaloacetate (OAA) (f) to 60% reduction in flow. C_c and C_m represent cytosolic and mitochondrial concentrations, respectively.

after ischemia). α -Ketoglutarate concentration increased by sevenfold in cytosol, but only 6% in mitochondria (Fig. 5e).

To investigate the impact of altered transport activity in M–A shuttle on cardiac metabolism in response to ischemic conditions, we simulated the metabolic response during ischemia with decreased transport rate and increased affinity coefficient. Our

results show that decreasing the normalized unidirectional transport rate coefficient by 50% or increasing the affinity coefficients by 200% had no significant effect on the cytosolic and mitochondrial redox states at a given level of myocardial ischemia, nor on the steady-state values of M–A shuttle flux (data not shown).

4. Discussion

Given the current experimental limitations, computational modeling with detailed M–A shuttle presentation provides an opportunity to gain insight into the role of M–A shuttle in regulating and coordinating metabolic activities between cytosolic and mitochondrial compartments in response to altered pathophysiological conditions. Such *in silico* experiments allow new hypotheses to be formulated that may eventually be tested by experimental means.

4.1. Model validation

To validate our current model, simulations were compared with data from *in vivo* experiments performed in pigs subjected to 60% reduction in coronary blood flow (Stanley et al., 1992; Salem et al., 2004). The model predictions were consistent with experimental data on glycogen concentration and lactate uptake/production (Fig. 2). The reduction in oxygen delivery leads to a decrease in oxidative phosphorylation and ATP production in mitochondria. As a result, anaerobic glycolysis and glycogenolysis increase. Our simulations confirmed a glycogen breakdown and a switch from net lactate uptake to release observed experimentally (Arai et al., 1991; Stanley et al., 1997). During ischemia, the accelerated glycolysis and reduced M–A shuttle flux (Fig. 5a) resulted in an elevated cytosolic redox state (Fig. 4a), leading to the conversion of pyruvate to lactate and, therefore, lactate accumulation. When glycogen storage is depleted, the cytosolic redox state and lactate efflux fall to a new steady state (Fig. 4a and 2b), as was found experimentally (Arai et al., 1991).

4.2. Localization of M–A shuttle

Our results suggest that the behavior of the dynamic response to altered metabolic conditions is different when different values of shuttle-associated effective volume were chosen. When the model assumed either a large or no subdomain for the M–A shuttle, there was a two-stage increase in the simulated dynamics of the cytosolic and mitochondrial redox states after the onset of ischemia (Fig. 3). However, with a much-reduced effective volume for the M–A shuttle-associated metabolites, the simulation showed a continuous increase in cytosolic and mitochondrial redox states at the onset of ischemia. To the best of our knowledge, the two-stage behavior during the abrupt transition from aerobic condition to ischemia has not been reported in literature. Our results may provide *in silico* evidence for the possibility of the spatial localization of M–A shuttle to a subdomain that spans the mitochondria and cytosol.

The concept of M–A shuttle localization is also consistent with the postulation of metabolic channeling of shuttle-associated metabolites from experimental findings. Aspartate aminotransferase has been reported to be firmly bound to inner membranes in guinea pig heart (Wit-Peeters et al., 1971). In addition, α -ketoglutarate dehydrogenase complex binds both aspartate aminotransferase and malate dehydrogenase to form a ternary complex that can enhance malate oxidation in the presence of malate and glutamate (Fahien et al., 1988, 1989). These multi-enzyme complexes can effectively increase the reaction rates by maintaining high local intermediate concentrations and reducing the transit time of intermediates between enzymes (Ovadi, 1991; Al-Habori, 1995; Mendes et al., 1995). Further, it also enhances the interaction between the TCA cycle and the M–A shuttle, therefore, allowing the metabolic status in the cytosol to be translated into the mitochondria and vice versa.

It is important to point out that the spatial localization of the M–A shuttle suggested by our current study is a functional rather than a physical compartmentation of the M–A shuttle. It is possible that the restricted effective volume of the shuttle may largely reflect the localization of the transporters in the mitochondria membrane, as shuttle-associated enzymes are abundant and readily available, especially in the mitochondria.

4.3. Mechanism for altered M–A shuttle flux during blood flow reduction

Consistent with previous experimental observations (Lewandowski et al., 1997), our simulation results indicate that ischemia impairs metabolic communication between cytosol and mitochondria by inducing a rapid reduction in M–A shuttle flux (Fig. 5a). This impairment is directly responsible for lactate accumulation and release due to reduced transport of cytosolic NADH into the mitochondria. To explore the mechanisms responsible for reduced M–A shuttle flux, we performed simulations with varied unidirectional transporter I (GLT-ASP transporter) activity, a rate-controlling step in M–A shuttle. The alterations in transporter activity was achieved by either decreasing the transport rate coefficient or increasing the transport affinity coefficients, representing either a decrease in protein expression level or an inhibition of substrate binding through allosteric modulation. Our simulations show that changes in transporter activity had no significant effects on the cytosolic and mitochondrial redox states during ischemia, nor on the steady-state values of M–A shuttle flux (data not shown). A closer examination of the shuttle-associated metabolites revealed that there were significant changes in the concentrations of these metabolites both in cytosol and mitochondria (Fig. 5b–f). Therefore, the decrease in M–A shuttle flux during ischemia is unlikely due to the modulation of the rate-controlling GLT-ASP transporter. Rather, it is through the redistribution of shuttle-associated metabolites across the mitochondrial membrane that such reduction is induced. Thus, the dramatic acceleration in glycolysis and lactate accumulation with the onset of ischemia is mediated by the redistribution of shuttle-associated metabolites in cytosolic and mitochondrial compartments in response to an increase in glycolytic NADH generation and decreased mitochondrial NADH oxidation by Complex I.

4.4. Dynamic responses of cytosolic and mitochondrial redox states to ischemia

The response of cytosol and mitochondria to ischemia showed different characteristics. Cytosolic redox state showed a biphasic transition to the new steady state, while mitochondrial redox state showed a rapid, step-wise increase that paralleled the change in blood flow. This difference suggests that regulation of the redox state is localized during ischemia. During ischemia, lower oxygen availability inhibits the rate of mitochondrial NADH oxidation through the electron transport chain and leads to a rapid mitochondrial NADH accumulation. Therefore, the blood flow reduction and the consequent changes in myocardial oxygen consumption determine the quick response of mitochondrial redox state. In contrast, the dynamic response of cytosolic redox state exhibits a biphasic behavior. Immediate changes in cytosolic redox state are determined primarily by accelerated glycolysis following ischemia and secondarily by altered M–A shuttle flux. Due to the decrease in M–A shuttle flux, transport of increased cytosolic NADH generated from the activation of glycolysis and glycogenolysis is significantly impaired, leading to progressive NADH accumulation and lactate production in the cytosol until

the glycogen pool is depleted. Following the depletion of endogenous glycogen, rate of glycolysis decreases, which gives rise to the partial restoration of cytosolic redox state due to reduced NADH production.

4.5. Model limitations and future directions

Our current model used a single Michaelis–Menten equation to describe the kinetics of the GLT-ASP transporters. It has been recognized that adult heart expresses two isoforms of GLT-ASP transporter, aralar1 and citrin (del Arco and Satrustegui, 1998; del Arco et al., 2000, 2002; Kobayashi et al., 1999). These two isoforms share strong similarity in their carrier sequence, with differences in the N-terminus, the calcium-binding site (del Arco et al., 2000). Studies with reconstituted liposomes and isolated mitochondria suggest that these two isoforms have very similar transport activities but different calcium activation kinetics (Contreras et al., 2007; Palmieri et al., 2001). Since the current study focused on the metabolic interaction between cytosol and mitochondria and the dynamic transition from normal conditions to ischemia, the approximation with one Michaelis–Menten equation is plausible when calcium regulation is not involved. However, the differentiation of the two carriers with distinct calcium regulation parameters may be necessary under other circumstances (e.g., exercise).

Our current model has focused on major metabolic pathways associated with oxidative metabolism and ATP generation. It is not an exhaustive model that incorporates all the pathways associated with cardiac metabolism. The model predicted a decrease in total aspartate concentration during ischemia, which is consistent with experimental data. The changes in glutamate and malate concentrations differ from those measured previously in isolated perfused rat hearts (Peuhkurinen et al., 1983). Such discrepancies may be due to the unphysiological metabolic conditions used in the previous study, where fatty acids, the primary substrate of the heart, were absent and glucose was the sole exogenous substrate. On the other hand, our model does not incorporate anaplerotic and cataplerotic pathways, specifically pyruvate carboxylation, which may effect malate concentration. Further, only transamination reactions directly involved in the M–A shuttle were considered by the current model. However, an increase in alanine concentration concurrent with the decrease in aspartate concentration, with no change in glutamate concentration, has been observed in glucose-perfused rat hearts. It is important to note that no changes in alanine or glutamate production were observed in the pig heart with a 60% reduction in coronary flow (Hacker et al., 1992), suggesting that observations in the isolated rat hearts may be due to the lack of physiological substrates.

Ischemia induces changes in ionic concentrations in both cytosol and mitochondria. While increased glycolysis and lactate accumulation cause intracellular pH to drop rapidly, inhibition of Na^+/K^+ ATPase due to declining ATP concentration leads to a rise in intracellular $[\text{Na}^+]$ and consequently an increase in $[\text{Ca}^{2+}]$ because of reduced activity in $\text{Na}^+/\text{Ca}^{2+}$ exchanger (Insarte et al., 2002). In addition, due to the rapid breakdown of Mg^{2+} -ATP, there is also an increase in intracellular $[\text{Mg}^{2+}]$ (Murphy et al., 1991). The regulatory roles of these ions, particularly Ca^{2+} , on energy metabolism have been extensively investigated. It has been shown that Ca^{2+} can rapidly activate ATP production via F_1F_0 -ATP synthase and several calcium-sensitive dehydrogenases that are responsible for NADH generation, including pyruvate dehydrogenase, isocitrate dehydrogenase and α -ketoglutarate dehydrogenase (Denton et al., 1988; McCormack and Denton, 1989; Territo et al., 2000). In our current study, alterations in enzymatic activity due to changes in ionic concentrations were not

incorporated in the model. As the current study focused on metabolic adaptations during ischemia where oxygen availability is the major rate-determining step in the early transition from normal to ischemic conditions, it is unlikely that changes in ionic concentrations would alter the results of current model simulation. However, for studies that investigate the effect of prolonged ischemia or post-ischemia reperfusion, it is important to take into consideration alterations in ion concentration and the consequent changes in enzymatic activity.

Incorporating major components of M–A shuttle into a model of cardiac metabolism yields more quantitative, mechanistic information than previously available. Although the current model has been partially validated with the glycolytic data (e.g., glycogen breakdown, lactate uptake and production, etc.), experimental data of M–A shuttle components are needed to directly validate model predictions of the metabolic interaction between cytosol and mitochondria. This requires the development of experimental techniques to assess metabolic communication between cytosolic and mitochondrial compartments in intact tissues. While measuring metabolite concentrations in these distinct compartments remains a challenge, dynamic ^{13}C NMR spectroscopy in perfused hearts has been shown to be sensitive to redox changes in cytosol (Yu et al., 1996). When combined with mathematical modeling of the labeling kinetics of ^{13}C -enriched metabolites, such an approach is expected to yield new insights into this important mechanism that regulates metabolic activities in both cytosol and mitochondria.

In conclusion, this study suggests that the redistribution of shuttle-associated metabolites across the mitochondrial membrane is the evident mechanism for reduced M–A shuttle flux in response to ischemia, which leads to accelerated glycolysis and lactate accumulation. In addition, it also provides *in silico* evidence of the localization of M–A shuttle in cardiomyocytes.

Acknowledgments

This research was supported by a grant from NIGMS-NIH (GM-66309) establishing the Center for Modeling Integrated Metabolic Systems (MIMS). Dr. Yu was supported by grants from NHLBI (HL73315 and HL86935). Dr. Stanley was supported by a grant from NHLBI (HL-74237).

Appendix A. Supplementary Materials

Supplementary data associated with this article can be found in the online version at doi:10.1016/j.jtbi.2008.05.033.

References

- Al-Habori, M., 1995. Microcompartmentation, metabolic channelling and carbohydrate metabolism. *Int. J. Biochem. Cell Biol.* 27, 123–132.
- Arai, A.E., Pantely, G.A., Anselone, C.G., Bristow, J., Bristow, J.D., 1991. Active downregulation of myocardial energy requirements during prolonged moderate ischemia in swine. *Circ. Res.* 69, 1458–1469.
- Caputo, M., Dihmis, W.C., Bryan, A.J., Suleiman, M.S., Angelini, G.D., 1998. Warm blood hyperkalaemic reperfusion ('hot shot') prevents myocardial substrate derangement in patients undergoing coronary artery bypass surgery. *Eur. J. Cardiothorac. Surg.* 13, 559–564.
- Contreras, L., Gomez-Puertas, P., Iijima, M., Kobayashi, K., Saheki, T., Satrustegui, J., 2007. Ca^{2+} activation kinetics of the two aspartate-glutamate mitochondrial carriers, aralar and citrin: role in the heart malate–aspartate NADH shuttle. *J. Biol. Chem.* 282, 7098–7106.
- Dawson, A.G., 1979. Oxidation of cytosolic NADH formed during aerobic metabolism in mammalian cells. *Trends Biochem. Sci.* 4, 171–176.
- del Arco, A., Satrustegui, J., 1998. Molecular cloning of Aralar, a new member of the mitochondrial carrier superfamily that binds calcium and is present in human muscle and brain. *J. Biol. Chem.* 273, 23327–23334.

- del Arco, A., Agudo, M., Satrustegui, J., 2000. Characterization of a second member of the subfamily of calcium-binding mitochondrial carriers expressed in human non-excitabile tissues. *Biochem. J.* 345 (Pt 3), 725–732.
- del Arco, A., Morcillo, J., Martinez-Morales, J.R., Galian, C., Martos, V., Bovolenta, P., Satrustegui, J., 2002. Expression of the aspartate/glutamate mitochondrial carriers aralar1 and citrin during development and in adult rat tissues. *Eur. J. Biochem.* 269, 3313–3320.
- Denton, R.M., Rutter, G.A., Midgley, P.J., McCormack, J.G., 1988. Effects of Ca^{2+} on the activities of the calcium-sensitive dehydrogenases within the mitochondria of mammalian tissues. *J. Cardiovasc. Pharmacol.* 12 (Suppl. 5), S69–S72.
- Fahien, L.A., Kmietek, E.H., MacDonald, M.J., Fibich, B., Mandic, M., 1988. Regulation of malate dehydrogenase activity by glutamate, citrate, α -ketoglutarate, and multienzyme interaction. *J. Biol. Chem.* 263, 10687–10697.
- Fahien, L.A., MacDonald, M.J., Teller, J.K., Fibich, B., Fahien, C.M., 1989. Kinetic advantages of hetero-enzyme complexes with glutamate dehydrogenase and the α -ketoglutarate dehydrogenase complex. *J. Biol. Chem.* 264, 12303–12312.
- Gibala, M.J., Tarnopolsky, M.A., Graham, T.E., 1997. Tricarboxylic acid cycle intermediates in human muscle at rest and during prolonged cycling. *Am. J. Physiol.* 272, E239–E244.
- Griffin, J.L., O'Donnell, J.M., White, L.T., Hajjar, R.J., Lewandowski, E.D., 2000. Postnatal expression and activity of the mitochondrial 2-oxoglutarate-malate carrier in intact hearts. *Am. J. Physiol. Cell Physiol.* 279, C1704–C1709.
- Hacker, T.A., Hall, J.L., Stone, C.K., Stanley, W.C., 1992. Alanine, glutamate, and ammonia exchanges in acutely ischemic swine myocardium. *Basic Res. Cardiol.* 87, 184–192.
- Inserte, J., García-Dorado, D., Ruiz-Meana, M., Padilla, F., Barrabes, J.A., Pina, P., Agullo, L., Piper, H.M., Soler-Soler, J., 2002. Effect of inhibition of $\text{Na}^{+}/\text{Ca}^{2+}$ exchanger at the time of myocardial reperfusion on hypercontracture and cell death. *Cardiovasc. Res.* 55, 739–748.
- Kobayashi, K., Sinasac, D.S., Iijima, M., Boright, A.P., Begum, L., Lee, J.R., Yasuda, T., Ikeda, S., Hirano, R., Terazono, H., Crackower, M.A., Kondo, I., Tsui, L.C., Scherer, S.W., Saheki, T., 1999. The gene mutated in adult-onset type II citrullinemia encodes a putative mitochondrial carrier protein. *Nat. Genet.* 22, 159–163.
- LaNoue, K.F., Williamson, J.R., 1971. Interrelationships between malate–aspartate shuttle and citric acid cycle in rat heart mitochondria. *Metabolism* 20, 119–140.
- LaNoue, K.F., Tischler, M.E., 1974. Electrogenic characteristics of the mitochondrial glutamate–aspartate antiporter. *J. Biol. Chem.* 249, 7522–7528.
- LaNoue, K.F., Schoolwerth, A.C., 1979. Metabolite transport in mitochondria. *Annu. Rev. Biochem.* 48, 871–922.
- LaNoue, K.F., Walajtys, E.L., Williamson, J.R., 1973. Regulation of glutamate metabolism and interactions with the citric acid cycle in rat heart mitochondria. *J. Biol. Chem.* 248, 7171–7183.
- LaNoue, K.F., Meijer, A.J., Brouwer, A., 1974. Evidence for electrogenic aspartate transport in rat liver mitochondria. *Arch. Biochem. Biophys.* 161, 544–550.
- Lewandowski, E.D., Yu, X., LaNoue, K.F., White, L.T., Doumen, C., O'Donnell, J.M., 1997. Altered metabolite exchange between subcellular compartments in intact postischemic rabbit hearts. *Circ. Res.* 81, 165–175.
- McCormack, J.G., Denton, R.M., 1989. The role of Ca^{2+} ions in the regulation of intramitochondrial metabolism and energy production in rat heart. *Mol. Cell Biochem.* 89, 121–125.
- Mendes, P., Kell, D.B., Westerhoff, H.V., 1995. A series of cases in which metabolic channelling can decrease the pool size at constant net flux in a simple dynamic channel. *Biochem. Soc. Trans.* 23, 287S.
- Murphy, E., Freudenrich, C.C., Lieberman, M., 1991. Cellular magnesium and Na/Mg exchange in heart cells. *Annu. Rev. Physiol.* 53, 273–287.
- Ovadi, J., 1991. Physiological significance of metabolic channelling. *J. Theor. Biol.* 152, 1–22.
- Palmieri, L., Pardo, B., Lasorsa, F.M., del, A.A., Kobayashi, K., Iijima, M., Runswick, M.J., Walker, J.E., Saheki, T., Satrustegui, J., Palmieri, F., 2001. Citrin and aralar1 are Ca^{2+} -stimulated aspartate/glutamate transporters in mitochondria. *EMBO J.* 20, 5060–5069.
- Panchal, A.R., Comte, B., Huang, H., Kerwin, T., Darvish, A., Des, R.C., Brunengraber, H., Stanley, W.C., 2000. Partitioning of pyruvate between oxidation and anaplerosis in swine hearts. *Am. J. Physiol. Heart Circ. Physiol.* 279, H2390–H2398.
- Panchal, A.R., Comte, B., Huang, H., Dudar, B., Roth, B., Chandler, M., Des, R.C., Brunengraber, H., Stanley, W.C., 2001. Acute hibernation decreases myocardial pyruvate carboxylation and citrate release. *Am. J. Physiol. Heart Circ. Physiol.* 281, H1613–H1620.
- Peuhkurinen, K.J., Takala, T.E., Nuutinen, E.M., Hassinen, I.E., 1983. Tricarboxylic acid cycle metabolites during ischemia in isolated perfused rat heart. *Am. J. Physiol.* 244, H281–H288.
- Purvis, J.L., Lowenstein, J.M., 1961. The relation between intra- and extramitochondrial pyridine nucleotides. *J. Biol. Chem.* 236, 2794–2803.
- Rupert, B.E., Segar, J.L., Schutte, B.C., Scholz, T.D., 2000. Metabolic adaptation of the hypertrophied heart: role of the malate/aspartate and α -glycerophosphate shuttles. *J. Mol. Cell Cardiol.* 32, 2287–2297.
- Safer, B., 1975. The metabolic significance of the malate–aspartate cycle in heart. *Circ. Res.* 37, 527–533.
- Safer, B., Smith, C.M., Williamson, J.R., 1971. Control of the transport of reducing equivalents across the mitochondrial membrane in perfused rat heart. *J. Mol. Cell Cardiol.* 2, 111–124.
- Salem, J.E., Cabrera, M.E., Chandler, M.P., McElfresh, T.A., Huang, H., Sterk, J.P., Stanley, W.C., 2004. Step and ramp induction of myocardial ischemia: comparison of in vivo and in silico results. *J. Physiol. Pharmacol.* 55, 519–536.
- Scholz, T.D., Koppenhafer, S.L., 1995. Reducing equivalent shuttles in developing porcine myocardium: enhanced capacity in the newborn heart. *Pediatr. Res.* 38, 221–227.
- Scholz, T.D., Koppenhafer, S.L., tenEyck, C.J., Schutte, B.C., 1998. Ontogeny of malate–aspartate shuttle capacity and gene expression in cardiac mitochondria. *Am. J. Physiol.* 274, C780–C788.
- Sluse, F.E., Ranson, M., Liebecq, C., 1972. Mechanism of the exchanges catalysed by the oxoglutarate translocatory of rat-heart mitochondria. Kinetics of the exchange reactions between 2-oxoglutarate, malate and malonate. *Eur. J. Biochem.* 25, 207–217.
- Stanley, W.C., Hall, J.L., Stone, C.K., Hacker, T.A., 1992. Acute myocardial ischemia causes a transmural gradient in glucose extraction but not glucose uptake. *Am. J. Physiol.* 262, H91–H96.
- Stanley, W.C., Lопасчук, G.D., Hall, J.L., McCormack, J.G., 1997. Regulation of myocardial carbohydrate metabolism under normal and ischaemic conditions. Potential for pharmacological interventions. *Cardiovasc. Res.* 33, 243–257.
- Stanley, W.C., Kivilo, K.M., Panchal, A.R., Hallowell, P.H., Bomont, C., Kasumov, T., Brunengraber, H., 2003. Post-ischemic treatment with dipyrucyl-acetyl-glycerol decreases myocardial infarct size in the pig. *Cardiovasc. Drugs Ther.* 17, 209–216.
- Taylor, S.W., Fahy, E., Zhang, B., Glenn, G.M., Warnock, D.E., Wiley, S., Murphy, A.N., Gaucher, S.P., Capaldi, R.A., Gibson, B.W., Ghosh, S.S., 2003. Characterization of the human heart mitochondrial proteome. *Nat. Biotechnol.* 21, 281–286.
- Territo, P.R., Mootha, V.K., French, S.A., Balaban, R.S., 2000. Ca^{2+} activation of heart mitochondrial oxidative phosphorylation: role of the $\text{F}_0\text{F}_1\text{-ATPase}$. *Am. J. Physiol. Cell Physiol.* 278, C423–C435.
- Wit-Peeters, E.M., Scholte, H.R., van den, A.F., de, N.I., 1971. Intramitochondrial localization of palmityl-CoA dehydrogenase, β -hydroxyacyl-CoA dehydrogenase and enoyl-CoA hydratase in guinea-pig heart. *Biochim. Biophys. Acta* 231, 23–31.
- Yu, X., White, L.T., Alpert, N.M., Lewandowski, E.D., 1996. Subcellular metabolite transport and carbon isotope kinetics in the intramyocardial glutamate pool. *Biochemistry* 35, 6963–6968.
- Zhou, L., Salem, J.E., Saidel, G.M., Stanley, W.C., Cabrera, M.E., 2005a. Mechanistic model of cardiac energy metabolism predicts localization of glycolysis to cytosolic subdomain during ischemia. *Am. J. Physiol. Heart Circ. Physiol.* 288, H2400–H2411.
- Zhou, L., Stanley, W.C., Saidel, G.M., Yu, X., Cabrera, M.E., 2005b. Regulation of lactate production at the onset of ischaemia is independent of mitochondrial $\text{NADH}/\text{NAD}^{+}$: insights from in silico studies. *J. Physiol.* 569, 925–937.
- Zhou, L., Cabrera, M.E., Okere, I.C., Sharma, N., Stanley, W.C., 2006. Regulation of myocardial substrate metabolism during increased energy expenditure: insights from computational studies. *Am. J. Physiol. Heart Circ. Physiol.* 291, H1036–H1046.